

# INSAR COHERENCE AND POLARIMETRIC PARAMETERS BASED CHARACTERIZATION OF FLOODED AREA - CASE STUDY OF A NATURAL WORLD HERITAGE SITE KAZIRANGA NATIONAL PARK

Dini Das A.S., Shashi Kumar, Arun Babu\*, Praveen K. Thakur

Indian Institute of Remote Sensing, Dehradun, Uttrakhand, India – dinidas94@gmail.com, shashi@iirs.gov.in,  
arunlekshmi1994@gmail.com, praveen@iirs.gov.in

## Commission V, SS: Disaster Monitoring, Damage Assessment and Risk Reduction

**KEYWORDS:** Flood, Polarimetric decomposition, Polarimetric classification, Interferometric coherence

### ABSTRACT:

Flood is a major threat to one of the UNESCO world heritage site of India-The Kaziranga National Park. Every year during the monsoon several hundreds of animals which include globally threatened species like single-horned Indian Rhinoceros of Kaziranga lose their lives due to the flood. The Synthetic Aperture Radar (SAR) can be used to monitoring the flood than the optical remote sensors because of their capability of all-weather and time-independent operability. The microwave L band is most suitable for the flood studies because of its higher penetration capability even through the vegetation. In this study, the advantages of SAR polarimetry and Interferometry of multi-temporal L band dual-pol data of ALOS PALSAR 2 were used to characterize the flooded area and also to monitor the flood extent. The H/A/Alpha decomposition gives a better characterization of the flooded area. The separability analysis is done with a different combination of decomposition parameters and the parameters having high-class separability between water and non-water areas are selected. Polarimetric classification using Random forest classifier is done on these selected decomposition parameters to classify the study into water and non-water areas. The classified images of different months before, during and after the flood time is used to quantitatively estimate the flood extent and for time series analysis. The Interferometric SAR coherence images along with the backscatter images are used to generate the RGB composites which also gives times series information on the flood impact.

### 1. INTRODUCTION

SAR Polarimetry is widely used nowadays for flood extent mapping and change detection because of the capability of the Microwaves to penetrate the clouds during the severe weather conditions like a flood. The availability of a large number of spatial and temporal SAR datasets from different spaceborne SAR sensors fuelled more research in this area.

India is one of the most flood-prone countries in the world. About 12% of the total area of India comes under the flood-prone zone ("Vulnerability Profile- National Disaster Management Authority," 2018). The Indo-Gangetic and Brahmaputra river basins are the most chronic flood-prone areas and are regarded as the worst flood affected region in the world. Because of this, the states of India -Uttar Pradesh, Assam, Bihar and West Bengal

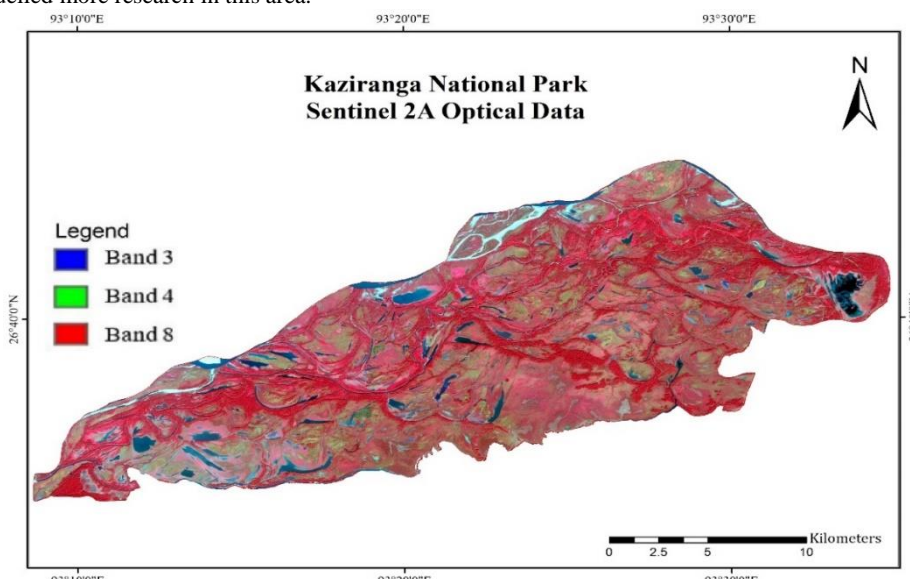


Figure 1. Standard False Colour Composite image of Study Area acquired using Sentinel-2A

are subjected to very disastrous flood in every year (Agarwal et al., 1991).

\* Corresponding author

The Standard False Colour Composite (SFCC) image of the Kaziranga National park is shown in figure 1. The SFCC image is created using the band 8, band 4 and band 3 images of the Sentinel-2A satellite, where band 8 is the Near Infrared (NIR) band with central wavelength of  $0.842\text{ }\mu\text{m}$ , band 4 is red band with central wavelength of  $0.665\text{ }\mu\text{m}$  and band 3 is green band with central wavelength of  $0.560\text{ }\mu\text{m}$ . The Kaziranga National Park, Assam is one of the world heritage site in India which was declared by UNESCO in 1985. Kaziranga is situated in the flood plains of river Brahmaputra. As per UNESCO- IUCN Enhancing Our Heritage Project report, there are about 34 beels within different ranges inside the Kaziranga National Park. Some of them are Kathphora, Mihibeel, Navbhangi, Borbeel, Sohola, Mohamari, Tinibeele, Laodubi, Daphlang, Borgugh, Tunikati, Baghbeel Ajgor, Monabeel, Karasing, Sukhani and Koladuwari (Mathur et al., 2007). During monsoon season flood is very common in this area and a major part of the park will become inundated. Mostly the flood season is from May to August. Due to the heavy rainfall on monsoon, the Brahmaputra along with other rivers in Kaziranga park (Dhansiri River, river Mora Diphlu) starts overflowing and makes the entire park flooded with water except for areas of higher elevation. The intensity of flood varies each year depending on the intensity of the rain. A number of chapories (river islands) which have been formed by silt depositions in the park helps the animals to stay safe from the flood (Kr, 2005). Also, they can migrate to the Karbi Anglong foothills in the flood season if they are getting sufficient time. During this migration, they are susceptible to hunting, hit by vehicles on the NH-37 adjacent to the park, or sometimes being attacked by the villagers. Any sudden rise in water level causes high mortality of the animals by drowning. Flood of 1988 and 1998 was reported as the worst years of Kaziranga in its flood history, where 652 animals recorded dead in flood of 1998. 540 animals, including 13 rhinos died in the flood of 2012. 70% of the National Park was flooded in 2016 and on 2017 flood event, about 361 animals drown in flood. Also, the flood destroyed the infrastructure of the park (Assam State Disaster Management Authority, 2017).

SAR polarimetry and interferometric coherence are used in this study to estimate the impact and flood extent at Kaziranga during 2016 to 2017 and to carry out the time series analysis and change detection.

## 2. DATASETS AND METHOD

### 2.1 Datasets

4 ALOS PALSAR-2 dual-Pol datasets acquired in the stripmap mode before and after the flood event is used for this study for polarimetric processing and coherence image generation. PALSAR-2 operates in L-band with 10-meter spatial resolution in stripmap mode. Sentinel-2A optical dataset of the study area acquired after the flood events is also used. The NIR, Red and Green bands of Sentinel-2A which are used in this study is having a spatial resolution of 10 meters. The details of the datasets are shown in Table 1.

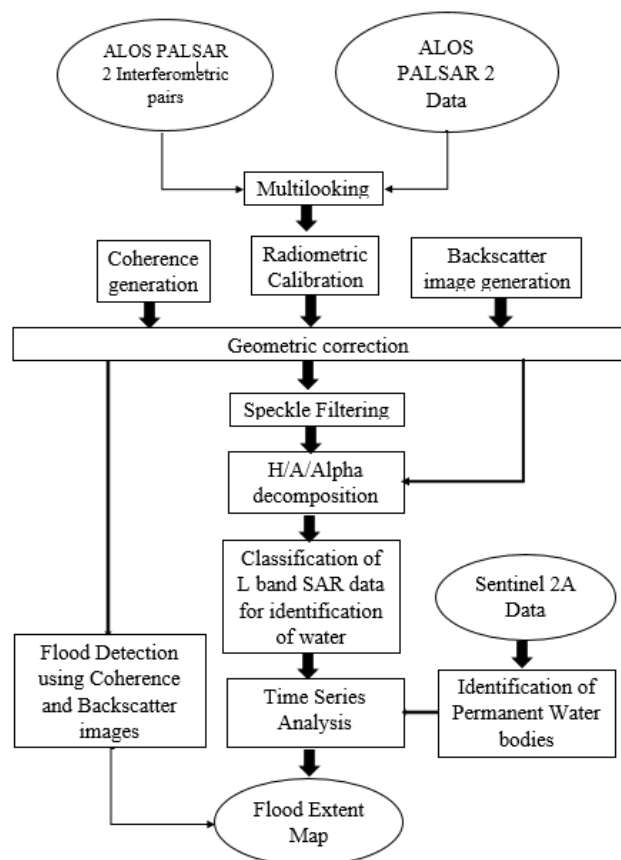
Sl no	Satellite	Date of Acquisition	Bands used
1	PALSAR-2	13/03/2016	HH, HV
2	PALSAR-2	03/07/2016	HH, HV
3	PALSAR-2	11/09/2016	HH, HV
4	PALSAR-2	29/01/2017	HH, HV
5	SENTINEL-2A	19/01/2017	NIR, Red, Blue

Table 1. Metadata of Datasets

### 2.2 Method

**2.2.1 Optical Data Processing:** The NIR, Red and Green bands of Sentinel-2A is stacked together to generate the Standard False Colour Composite (SFCC) images to distinguish different land use land cover in the image. The entire scene was subsetted using the boundary shapefile of Kaziranga National Park. In order to identify the water bodies in the study area, the subsetted image is then reclassified.

**2.2.2 SAR data processing:** The SLC datasets of ALOS PALSAR-2 is first multilooked to generate square pixels and to reduce the speckle present. After multilooking radiometric calibration is done to remove the gain errors present in the datasets so that the pixel values of the image actually represents the radar backscattering of the target on the ground. Geometric correction is applied next to orient the image to exactly fit to the terrain. Speckle filtering using  $5 \times 5$  Refined Lee filter is then applied to remove the speckles. After this initial pre-processing steps the polarimetric and coherence processing is done as per the flowchart is shown in Figure 2.



Polarimetric decomposition is done on the pre-processed SAR

Figure 2. Process Flowchart

datasets. The decomposition of SAR data allows determining the scattering mechanism within the pixels which helps in the feature identification. In this study, an Eigenvector Eigenvalue based decomposition technique called H/A/Alpha decomposition is used. It gives different decomposition parameters. For the Dual polarization data (HH and HV) we get a coherency matrix of  $2 \times 2$  in the form (Cloude, 2007; Pottier et al., 1997):

$$[J_H] = \begin{bmatrix} \langle S_{HH} S_{HH}^* \rangle & \langle S_{HH} S_{HV}^* \rangle \\ \langle S_{HV} S_{HH}^* \rangle & \langle S_{HV} S_{HV}^* \rangle \end{bmatrix} \quad (1)$$

As per the Eigenvalue Eigenvector based decomposition theorem, a 3x3 coherency matrix T can be decomposed as (Cloude et al., 1997; Cloude, 2007; Pottier et al., 1997):

$$T = U \Sigma U^{-1} \quad (2)$$

$$\Sigma = \begin{bmatrix} \lambda_1 & 0 & 0 \\ 0 & \lambda_2 & 0 \\ 0 & 0 & \lambda_3 \end{bmatrix} \quad U = [U_1 \quad U_2 \quad U_3]$$

Where  $\Sigma$  contains the Eigenvalues and U contains the Eigen Vectors. This matrix can be physically interpreted as statistical independence between a set of target vectors. The Decomposition parameters obtained from the H/A/Alpha decomposition are Entropy, Anisotropy, Alpha, Alpha 1, Alpha2, Eigen Values (L1, L2), Pseudo Probabilities (P1, P2), Delta, Delta 1, Delta , Lambda, Combinations of Entropy (H) and Anisotropy (A) and Shannon Entropy.

The eigenvalues ( $\lambda_i$ ) and the eigenvectors are the primary parameters of the Eigen decomposition. The value of the eigenvalue gives the importance of the corresponding eigenvector or scattering mechanism. Lambda ( $\lambda$ ) defined as nonnegative real eigenvalues of the diagonal matrix. The pseudo probability parameters  $p_i$ , are the probability of the eigenvalue ( $\lambda_i$ ), which represent the relative importance of this eigenvalue respect to the total scattered power (Yonezawa et al., 2012).

$$p_i = \frac{\lambda_i}{\sum_{k=1}^3 \lambda_k} \quad (3)$$

Entropy (H), Anisotropy (A) and Alpha ( $\alpha$ ) are the secondary parameters of this decomposition. Entropy describes the degree of statistical disorder of each target (Yonezawa et al., 2012).

$$H = - \sum_{i=1}^n p_i \ln p_i \quad (4)$$

When  $H \rightarrow 0$ :

$$\lambda_1 = \text{SPAN}$$

$$\lambda_2 = \lambda_3 = 0$$

The Anisotropy (A) is complementary to the entropy and it measures the relative importance of the second and the third eigenvalues of the Eigen decomposition (Yonezawa et al., 2012).

$$A = \frac{\lambda_2 - \lambda_3}{\lambda_2 + \lambda_3} \quad (5)$$

Anisotropy cannot be interpreted separately from the entropy. So we can use different combinations between the entropy and the anisotropy.

Alpha ( $\alpha$ ) angle gives the dominant scattering mechanism for each pixel (Yonezawa et al., 2012).

$$\underline{\alpha} = \sum_{i=1}^3 p_i \alpha_i \quad (6)$$

Where

$\alpha \rightarrow 0$ : The scattering corresponds to surface scattering

$\alpha \rightarrow \pi/4$ : The scattering corresponds to volume scattering.

$\alpha \rightarrow \pi/2$ : The scattering corresponds to double-bounce scattering.

The Shannon entropy (SE) is the sum of two contributions related to the intensity (SEI) which depends on the total backscattering and Polarimetry (SEP) which depends on the degree of polarization of SAR data (Refregier et al., 2006). From this parameter, we can determine the fractional contribution of the polarimetry and intensity in entropy.

$$SE = SEI + SEP \quad (7)$$

The fluctuating random variables have a high value of Shannon entropy, while the quasi-deterministic random variables have relatively low value (Cloude, 2007).

After obtaining the decomposition parameter images for each image, separability analysis is done to select the parameters which give maximum separability between water and non-water areas. The separability analysis is done using both Euclidian distance method and with the minimum, maximum, mean and standard deviation values of the water and non-water areas.

Polarimetric classification is done on the decomposition parameters having the maximum separability between water and non-water areas. The classification groups the pixels of the image into different classes. The classification techniques can be classified broadly into supervised classification and unsupervised classification. Random forest classification, which is a supervised classification technique was used (Lee et al., 2017).

After classifying the decomposition parameter images accuracy assessment is done. Accuracy assessment is an important procedure after the image classification which is to assess how well the classification is done. When a pixel (or feature) belonging to one category is assigned to another category, the Classification error can occur. Thus the accuracy of the classification can be done by comparison of the classified image with reference data (ground truth data with GCPs, high-resolution satellite images or a pre-existing classified image which is considered to be accurate). The confusion matrix is the most commonly used accuracy assessment technique. Using the confusion matrix we can determine the overall accuracy, user accuracy and producer accuracy of the classification.

The classified images of different time periods are used to generate the time series map to estimate the flood extent.

SAR coherence ( $\gamma$ ) can be used as a means of change detection of a terrain. Coherence will be high for areas on the ground where no change occurred between two time periods. The coherence of two SAR images  $V_1$  and  $V_2$  can be computed as follows:

$$\gamma = \frac{E\langle V_1 V_2^* \rangle}{\sqrt{\langle |V_1|^2 \rangle \langle |V_2^*|^2 \rangle}} \quad (10)$$

Where,

$E\langle \rangle$  indicates the expected value which is in practice approximated with a sampled average and  $*$  represents the complex conjugate (Dellepiane et al., 2000).

For comparing and monitoring the presence of water in different times, the RGB composite of coherence and the backscatter of respective images were created.

### 3. RESULTS

The ALOS PALSAR-2 datasets and Sentinel-2A datasets are processed using the methodology described in the previous section to estimate the impact of the flood on the study area.

Initially, the SFCC image of the study area acquired after the flood event generated from the Sentinel-2A dataset is reclassified in order to identify the permanent water bodies. The reclassified image is shown in Figure 3. The total area of the permanent water bodies calculated from the classified image is 2756.16 ha. The decomposition parameter images generated after polarimetric decomposition are shown in Figure 4.

The decomposition parameters Eigenvalues (figure 4h & figure 4i), normalized Shannon entropy parameters (figure 4d & figure 4e), and lambda (figure 4g) is much effective in giving a distinct view of the water and non-water area in the scene than the other decomposition parameters like alpha, delta, pseudo probability values and anisotropy.

To statistically estimate the separability between water and non-water areas separability analysis is done for the decomposition parameters by calculating its minimum value, maximum value, the mean and standard deviation for water and non-water areas. From Figure 5 it can be seen that Lambda is showing the high difference between the mean and standard deviation between the two classes and it can be used to distinguish between the water and non-water (figure 5c). The normalized Shannon entropy

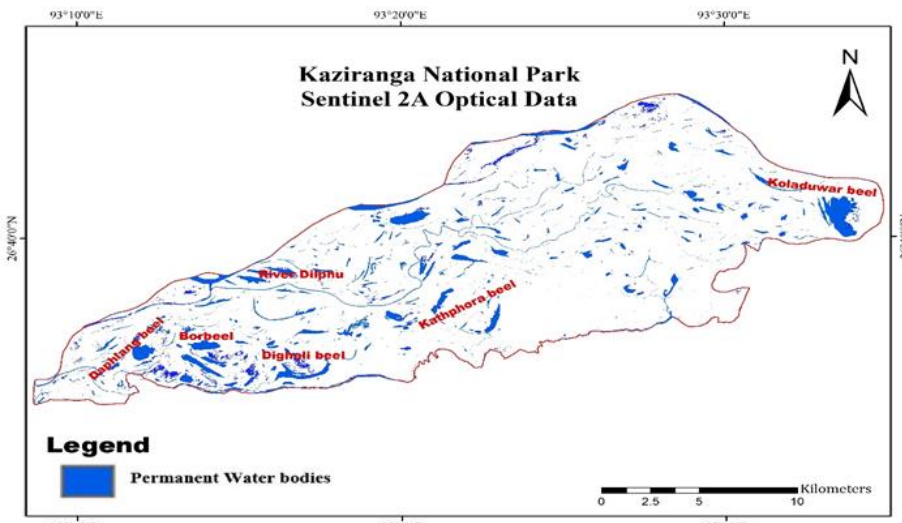


Figure 3. Classified image of Sentinel 2A data on 19/01/2017

parameters show a very good separability (figure 5b). The mean, minimum, standard deviation and a maximum of water for both the Shannon entropy decomposition parameters are zero as seen in the figure. The Eigenvalue parameters L1 and L2 are also giving much distinct values for water and non-water by which their separability becomes easier (figure 5a & b).

Separability analysis using Euclidian distance method is done using the Eigenvalue parameters, Lambda and Shannon entropy parameters to estimate which combination of these bands can give maximum separability so that efficient polarimetric classification can be done using the best possible combination ensuring high accuracy.

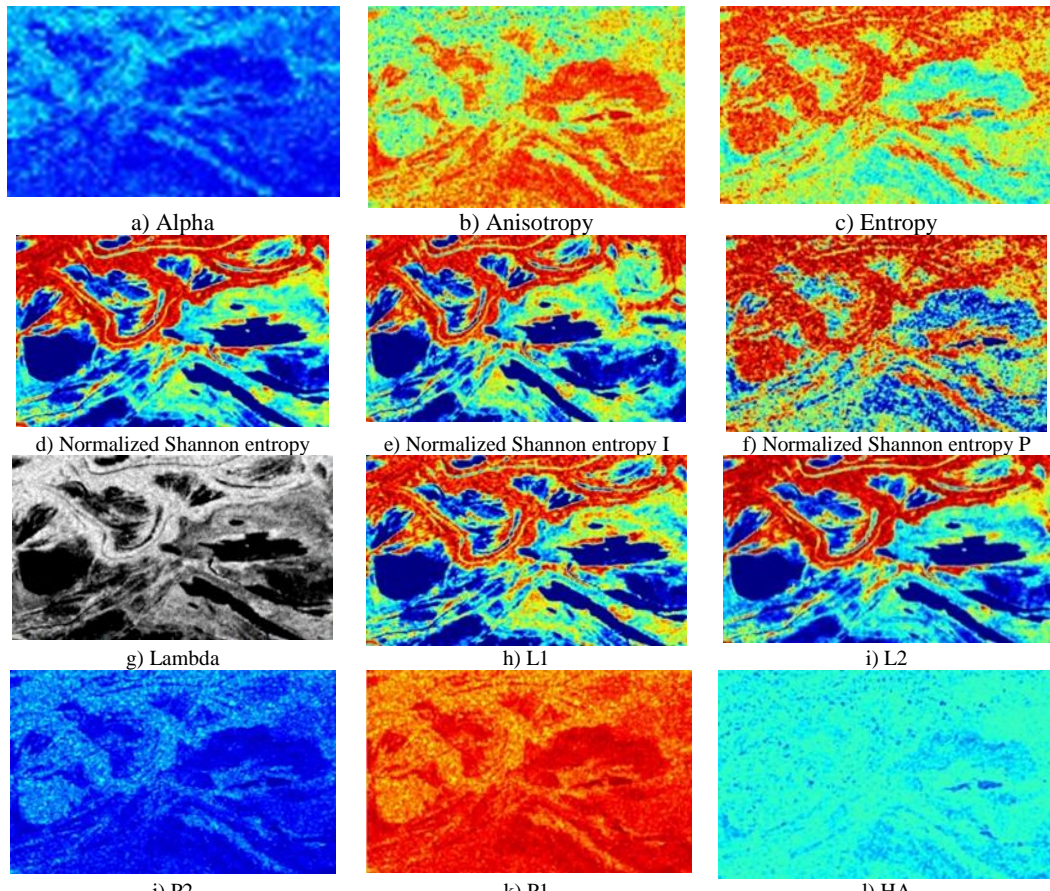


Figure 4. Decomposition parameters for a selected region of the study area

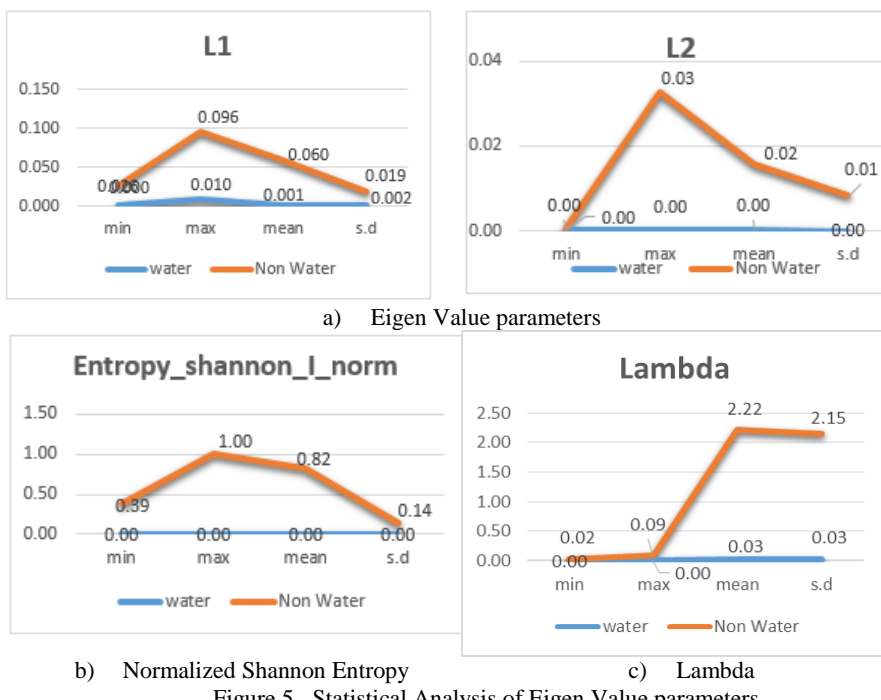


Figure 5. Statistical Analysis of Eigen Value parameters

From the figure 6 showing the feature spaces obtained through Euclidian distance separability analysis, it can be seen that the band combination of Normalized Shannon entropy with L1, L2 & Lambda, combination of Normalized Shannon entropy I with L2 and combination of L2 with L1 & Lambda gives maximum

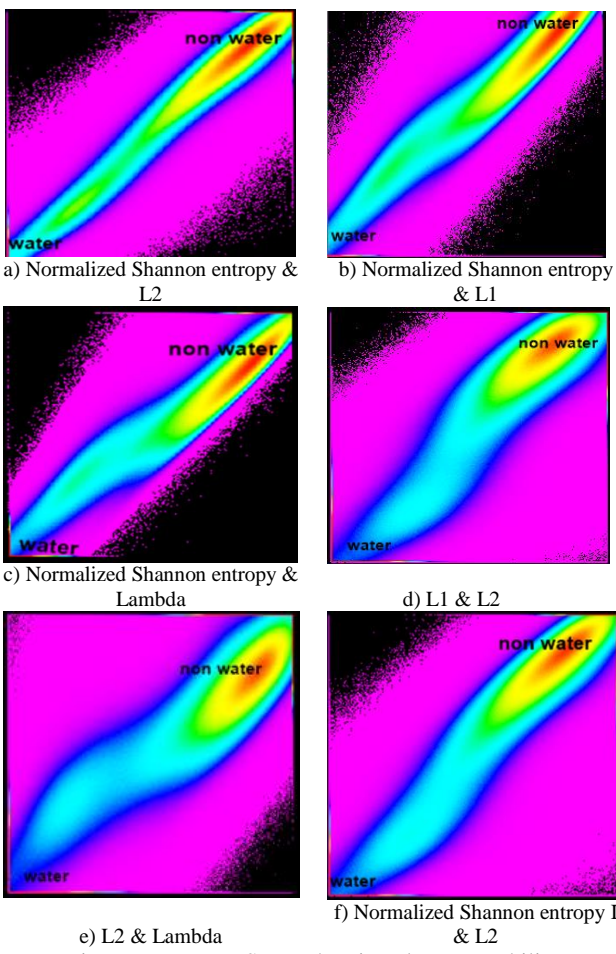


Figure 6. Feature Space showing class separability

separability between the classes compared to other possible combinations, because the cluster centre of the classes can be clearly identified.

The result of separability analysis for classes water and non-water using Euclidean distance measurement is given in table 2. From the separability analysis, it can be found that the Eigenvalue parameter L2 has higher separability between the two classes: water and non-water. Along with the decomposition parameters, the backscatter images also give better separability of water from other features in the image.

For the classification of the study area, the Random Forest Classification method is used. The decomposition parameters used for polarimetric classification are Normalized Shannon Entropy, Normalized Shannon Entropy I, Eigen Value Parameters L1, L2 and Lambda.

The Classified outputs of Random Forest Classifier are shown in Figure 7. Figure 7a shows the classified image before flood on 13/03/16. The permanent water bodies inside the Kaziranga National Park can be seen in the figure.

In the classified image of 03/07/16 (figure 7b), the occurrence of the flood is clearly visible. Most of the beels started overflowing which inundates the surrounding areas. The total area of water bodies in this period increased to 6942.266 ha.

Band	Separability (Euclidian Distance)
Normalized Shannon Entropy	218
Normalized Shannon Entropy I	212
L1	208
L2	221
Lambda	206

Table 2. Separability Analysis

Even During September, the park remains flooded. The overflowing of River Brahmaputra to its floodplain can also see in the classified image (figure 7b). Flood water from the flooded highlands, mostly from the southern part of Kahora range were receded and the total area of water bodies reduced to 6114.838 ha.

In the month of January 2017, the park has been completely recovered from the flood (figure 7d). The total area of water body became 2561.536 ha which is comparable to the area of permanent water bodies in the park (figure 7a).

Accuracy assessment is done for all the classified images. The figure 7a is classified with an overall accuracy of 95.86%. The

image of 03/07/16 (figure 7b) is classified with an overall accuracy of 97.47% with a comparatively less user accuracy of water of 90.73%. The image of 11/09/16 (figure 7c) is classified with an overall accuracy of 98.37% and achieved 100% user accuracy of non-water and producer accuracy of water. Image of 29/01/17 (figure 7d) was classified with an overall accuracy of 96.89%. The result of accuracy assessment shows all the maps were classified with high overall accuracy.

When the flood entered the park in July due to heavy rainfall it became 6942.26 ha. The area has been increased by 5209.93 ha shown in green colour. The Agratoli range of east and Buraphahar & Bagori Range in the west of the park were inundated due to the overflowing of the beels. The northern part was submerged by the overflowing of river Brahmaputra. The regions adjacent to the Brahmaputra remain flooded in September due to the river overflow is shown in red colour. In some part of the area, the

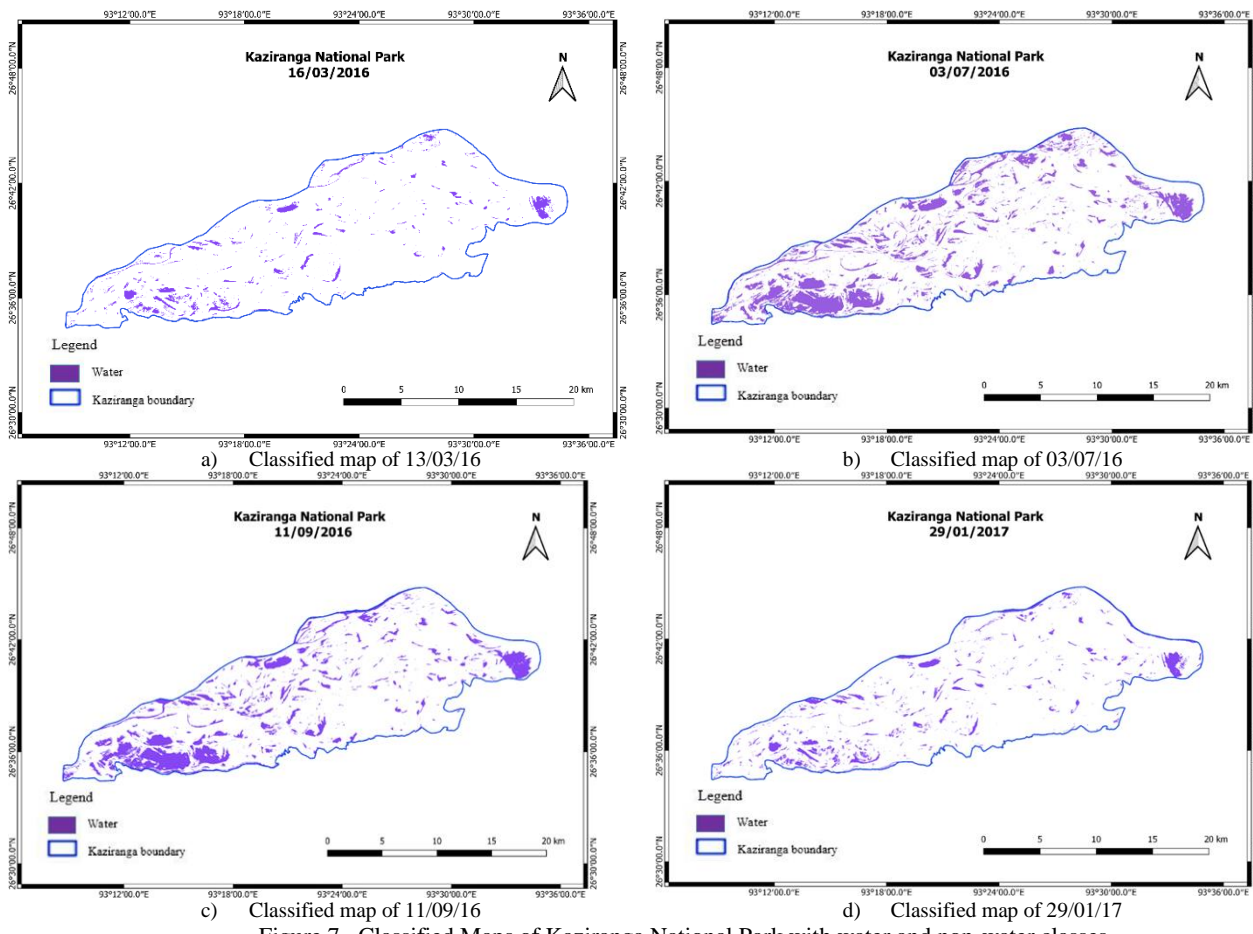


Figure 7. Classified Maps of Kaziranga National Park with water and non-water classes

The classified images of Kaziranga national park during different times is used for time series analysis to estimate the flood extent. From figure 8 it can be seen that on 13/03/16, the total area of water bodies in the park was 1732.33 ha shown in blue colour.

extent of water has been increased while in some southern parts the water has been started receding.

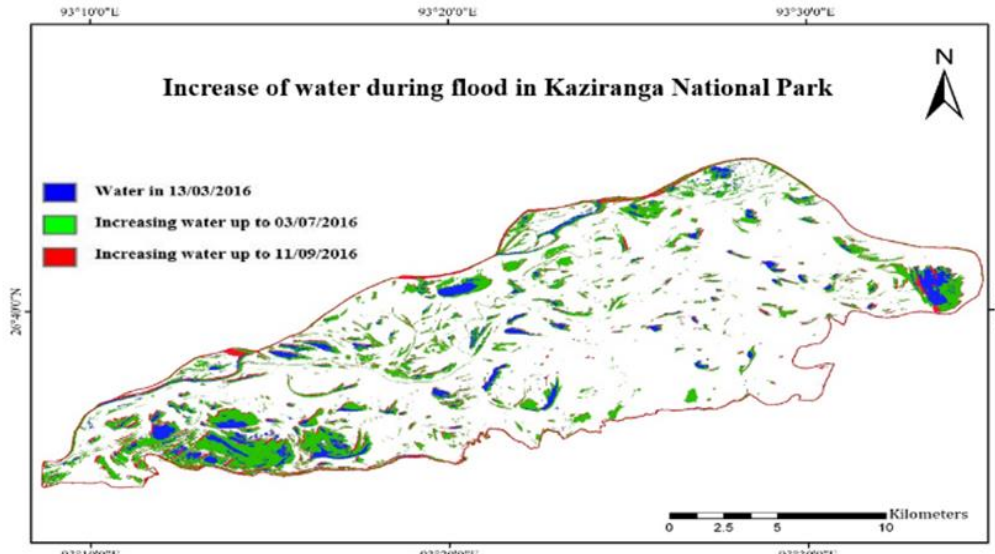


Figure 8. The increase of water during a flood in Kaziranga National Park

This contribution has been peer-reviewed. The double-blind peer-review was conducted on the basis of the full paper.  
<https://doi.org/10.5194/isprs-annals-IV-5-265-2018> | © Authors 2018. CC BY 4.0 License.

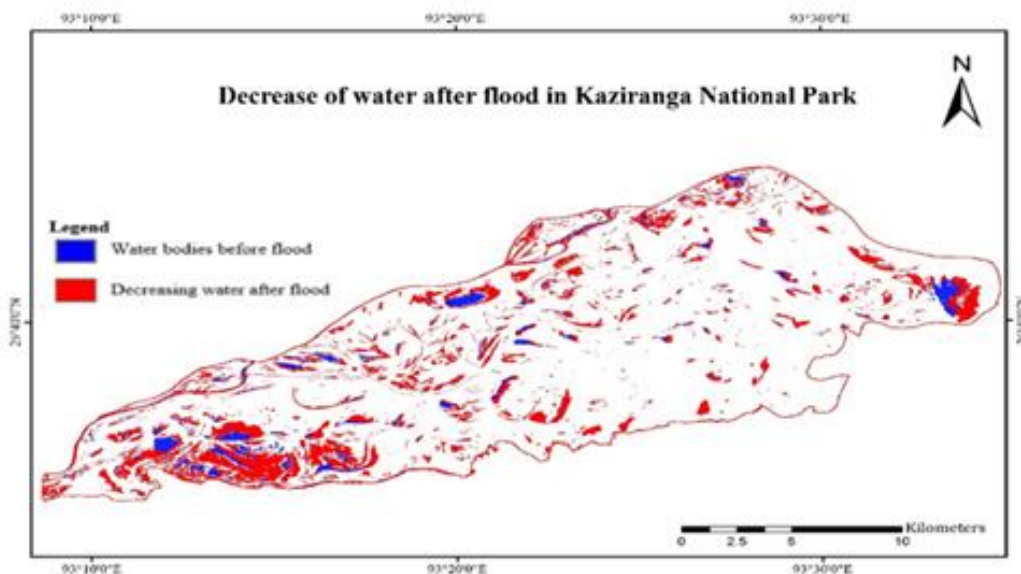


Figure 9. The decrease of water flood in Kaziranga National park

Figure 9 shows the decrease in water after the flood. After the flood event, the total area of water bodies decreased by 4380.73 ha and it became 2561.536 ha in January 2017. Even after the end of monsoon, the area of water is more than that of in March. Now the water flow of river dilphu and river Brahmaputra constrained to its river channel.

The coherence is the measure of similarity of backscatter from the interferometric pair images. Thus it can give valuable information regarding the change occurred in the area during the time interval of acquisition of the interferometric pairs. Use of coherence information will give an overview of how much the area get affected by the flood. The image on 13th March 2016 is a pre-flood image. The images of 3rd July 2016, 11th September 2016 and 29th January 2017 are post flood images. Different combinations of these images were used to estimate the coherence. The following images are generated by the RGB composite of coherence along with the respective backscatter images of different times (Pre-flood and post-flood).

In the images of 13/03/16 & 03/07/16 and 13/03/16 & 11/09/16 (figure 10), areas coloured with shades of red represent areas having high coherence before and after the flood with a maximum value of 0.44 and 0.42 respectively. The green channel has backscatter intensity before the flood. Thus it represents areas which were land before the flood and which became flooded after the flood. Because they are having low intensity (after the flood) in the blue channel they appear green. The blue colour represents areas having high backscatter in the blue channel.i.e, areas which are less or not affected by the flood. The Koladuwar lake in the eastern range, Kathpora beel in the Central range, Daphlang beel, borbeel and dighali beel in the western and far western range of Kaziranga is the main source of flooding in these ranges when high rainfall occurred during monsoon(June to September). The northern part of Kaziranga is submerged during this season mainly from the overflowing of river Brahmaputra.

From figure 11, it can be seen that the areas which were land on 13th March 2016 but have water on 29th January 2017 appears in green as in some northern parts of the study area, which are adjacent to the river Brahmaputra. There are areas with a high coherence which seen as brightly coloured in the image.

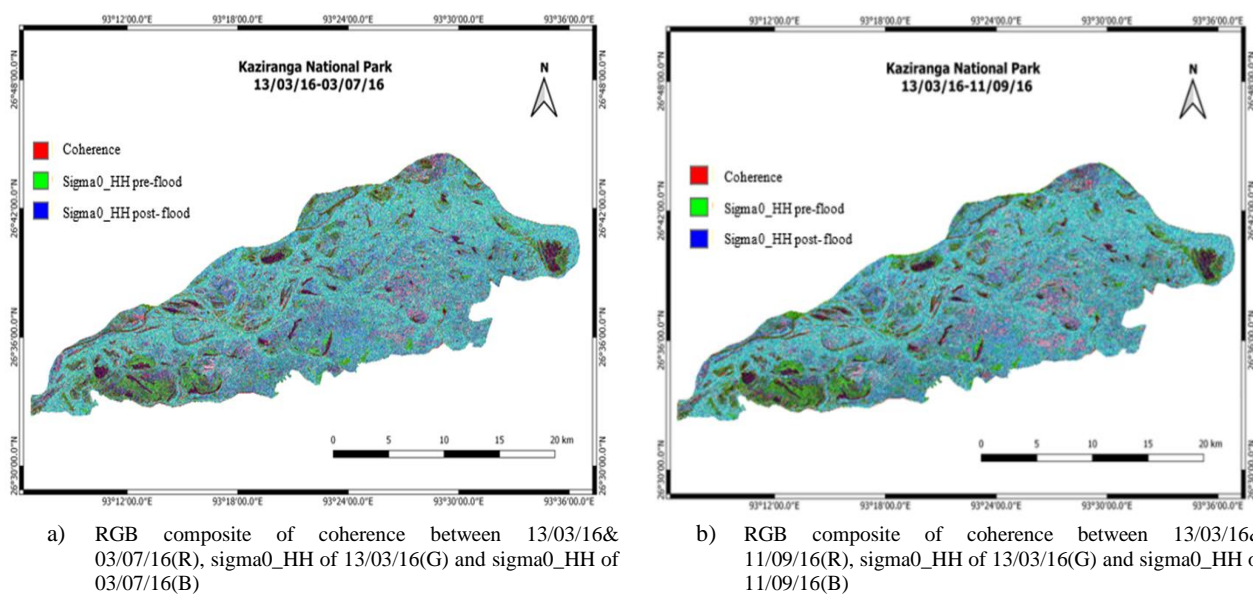


Figure 10. RGB composite Images

The coherence of the study area ranges from 0.01 to 0.46. The area around borbeel and daphlang beel in the western part possess high coherence that indicates the complete recovery of this area from the flood.

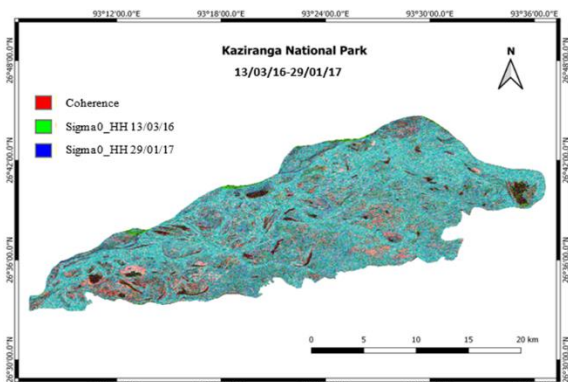


Figure 11. RGB composite of coherence between 13/03/16 & 29/01/17 (R), sigma0\_HH of 13/03/16 (G) and sigma0\_HH of 29/01/17 (B)

#### 4. CONCLUSION

Polarimetric parameters retrieved through polarimetric decomposition of dual-band ALOS PALSAR-2 L-band datasets were used in this study for polarimetric characterization of the study area. The separability analysis is done on the polarimetric decomposition parameters generated to identify the parameters which can give better discrimination between water and non-water areas. By examining all the decomposition parameters it is found that Normalized Shannon Entropy, Normalized Shannon Entropy I, Eigen Value Parameters L1, L2 and Lambda were the parameters having maximum separability between water and non-water pixels. Polarimetric classification is done using this parameter. The classified results obtained were able to clearly distinguish the water bodies. Different pairs of datasets are coregistered and stacked together to generate the interferometric coherence images. The coherence images were used to generate the RGB Composite images together with the backscatter images of pre-flood and post-flood time. The time series analysis of the flood impact is done using the classified images and RGB composite images of different time periods. The quantitative analysis using the time series data showed that before the impact of flood the total area of the water bodies at the study area was 2756.16 ha and it increased up to a maximum of 6942.26 during the flood time indicating the severe impact of the flood to the park. By the month of January 2017, the total water body area decreased to 2561.53ha indicating the complete recovery of the study area from the flood.

#### ACKNOWLEDGMENTS

We express our sincere gratitude to European Space Agency (ESA) for providing the SNAP and PolSAR Pro software capable of interferometric and polarimetric processing. We also express our sincere thanks to JAXA for providing the ALOS PALSAR-2 datasets under the proposal number 1408 of RA4 with the title Hydrological Parameter retrieval and glacier dynamics study with L-band SAR data. We are grateful to Indian Institute of Remote Sensing, Dehradun for providing all the support and infrastructure required for carrying out this research.

#### REFERENCES

- Agarwal, A., Sunitha, N., 1991. Floods, Flood Plains and Environmental Myths, State of India's environment. Centre for Science and Environment.
- Assam State Disaster Management Authority, 2017. Flood Report [WWW Document]. Assam State Disaster Manag. Auth. URL <http://asdma.gov.in/reports.html> (accessed 7.28.18).
- Cloude, S., Pottier, E., 1997. An entropy based classification scheme for land applications of polarimetric SAR. IEEE Trans. Geosci. Remote Sens. 35, 68–78. <https://doi.org/10.1109/36.551935>
- Cloude, S.R., 2007. The Dual Polarisation Entropy / Alpha Decomposition, in: Proceedings of the 3rd International Workshop on Science and Applications of SAR Polarimetry and Polarimetric Interferometry. pp. 1–6.
- Dellepiane, S.G., Bo, G., Monni, S., Buck, C., 2000. SAR images and interferometric coherence for flood monitoring. IGARSS 2000. IEEE 2000 Int. Geosci. Remote Sens. Symp. Tak. Pulse Planet Role Remote Sens. Manag. Environ. Proc. (Cat. No.00CH37120) 6, 2608–2610. <https://doi.org/10.1109/IGARSS.2000.859656>
- Kr, M.M., 2005. Improving Protection and Building Capacity of Staff At Kaziranga National Park.
- Lee, S., Kim, J.C., Jung, H.S., Lee, M.J., Lee, S., 2017. Spatial prediction of flood susceptibility using random-forest and boosted-tree models in Seoul metropolitan city, Korea. Geomatics, Nat. Hazards Risk 8, 1185–1203. <https://doi.org/10.1080/19475705.2017.1308971>
- Mathur, V.B., Choudhary, B.C., Vasu, N.K., 2007. UNESCO-IUCN Enhancing Our Heritage Project: Monitoring and Managing for Success in Natural World Heritage Sites. Assam, India.
- Pottier, E., Cloude, S.R., 1997. Application of the << H/A/alpha >> polarimetric decomposition theorem for land classification, in: Wideband Interferometric Sensing and Imaging Polarimetry. pp. 132–143. <https://doi.org/10.1117/12.278958>
- Refregier, P., Morio, J., 2006. Shannon entropy of partially polarized and partially coherent light with Gaussian fluctuations. J Opt Soc Am A Opt Image Sci Vis 23, 3036–3044. [https://doi.org/117913 \[pii\]](https://doi.org/117913 [pii])
- Vulnerability Profile- National Disaster Management Authority [WWW Document], 2018. . Natl. Disaster Manag. Auth. URL <https://ndma.gov.in/en/vulnerability-profile.html> (accessed 7.28.18).
- Yonezawa, C., Watanabe, M., Saito, G., 2012. Polarimetric decomposition analysis of ALOS PALSAR observation data before and after a landslide event. Remote Sens. 4, 2314–2328. <https://doi.org/10.3390/rs4082314>